or quasibound states, and that therefore the resonance level density does not keep increasing exponentially at higher energies.[9] Similarily, there is therefore no reason to expect that cross-section fluctuations due to resonance terms in the S matrix continue to very high energies.

---

*Work performed under the auspices of the U. S. Atomic Energy Commission.

[1]E. P. Wigner and L. Eisenbud, Phys. Rev. 72, 29 (1947).
[2]T. Ericson, Advan. Phys. 9, 425 (1960).
[3]K. Takeuchi and P. A. Moldauer, following paper Phys. Rev. C 2, 925 (1970).
[4]C. Bloch and V. Gillet, Phys. Letters 16, 62 (1965); H. A. Weidenmüller, Nucl. Phys. 75, 189 (1966); W. MacDonald and A. Mekjian, Phys. Rev. 160, 730 (1967).
[5]K. W. McVoy, Ann. Phys. (N.Y.) 43, 91 (1967).
[6]H. M. Nussenzveig, Nucl. Phys. 11, 499 (1959).
[7]J. Humblet, Mem. Soc. Roy. Sci. Liege 4, 12 (1952); T. Regge, Nuovo Cimento 8, 671 (1958).
[8]C. Mahaux and H. A. Weidenmüller, Phys. Rev. 170, 847 (1968).
[9]H. A. Weidenmüller, Phys. Letters 10, 331 (1964).

PHYSICAL REVIEW C VOLUME 2, NUMBER 3 SEPTEMBER 1970

R-Matrix Shell-Model Calculations of Scattering and Reaction Cross Sections*

K. Takeuchi and P. A. Moldauer
Argonne National Laboratory, Argonne, Illinois 60439
(Received 25 February 1970)

The Wigner-Eisenbud R-matrix theory is applied to the calculation of neutron total and inelastic scattering cross sections for a system consisting of two neutrons interacting with an inert ^{16}O core through a spherically symmetric Woods-Saxon potential and interacting with each other through a δ-function force. The calculational method employed has the advantages that it includes the effects of shell-model configurations in which both neutrons are unbound, that it presents no obstacles to inelastic or reaction calculations, that it permits antisymmetrization of the compound space wave functions, and that it requires only one shell-model diagonalization for the computation of cross sections up to 5-MeV neutron energy. Use of antisymmetrized wave functions is shown to reduce substantially the number of compound-nucleus resonances and to reduce the magnitude of the inelastic cross section. By the correct calculation of the distant resonance contribution to the R matrix, it is shown that the calculated cross sections are independent of the choice of channel radii. The application of the method to more complex systems with larger numbers of neutrons as well as protons and holes and also with direct coupling between channels is discussed. A selection rule encountered in the calculations suggests a possible J^{π} dependence of the absorptive part of the optical-model potential.

I. INTRODUCTION

The nuclear shell model is the basic theoretical tool for the description of atomic nuclei and has been used to calculate the properties of nuclear bound states. More recently, there has been considerable interest in the application of the shell model to the calculation of nuclear continuum states.[1] This paper deals with the analysis of the R-matrix method for the application of the shell model to nuclear cross-section calculations.

A bound-state shell-model calculation proceeds by the following five steps:

(1) A single-particle potential U is chosen. Most simply this is a spherically symmetric harmonic-oscillator plus spin-orbit potential.

(2) The single-nucleon spectrum of U is calculated by solving the single-particle Schrödinger equation

$$[K+U]\phi_{nljm}=E^{\mathrm{SP}}_{nlj}\phi_{nljm}\,, \tag{1}$$

where K is the kinetic-energy operator, and ϕ_{nljm} is the single-nucleon state with principal quantum numbers n, orbital and total angular momentum quantum numbers l, j, and z-component m.[2] The energy of the single-particle state ϕ_{nljm} is denoted by E^{SP}_{nlj}. The ϕ_{nljm} are orthonormal.

(3) A set of N-nucleon independent-particle states or configurations $|pJM\rangle$ is formed as the antisymmetrized product of N single-particle states, cou-

pled to total angular momentum quantum numbers J, M.

$$|pJM\rangle = C_p A\left[\prod_{i=1}^{N} \phi_{n_i l_i j_i m_i}\right]_{JM}, \tag{2}$$

where C_p is the appropriate normalization constant and A indicates antisymmetrization of the product.

(4) The shell-model Hamiltonian is constructed by adding to $K+U$ a two-body interaction V acting between all pairs of nucleons:

$$H = K + U + V. \tag{3}$$

(5) The matrix of H with respect to a limited part of the independent-particle configurations is formed,

$$\langle pJM|H|p'JM\rangle,$$

and diagonalized. Its eigenvalues are the energies $E_{\mu JM}$ of the shell-model states, and the corresponding eigenvectors give the expansion coefficients of the shell-model wave functions $|\mu JM\rangle$ in terms of the independent-particle basis states $|pJM\rangle$.

The above procedure yields only discrete states. In order to calculate cross sections, it is necessary to modify the procedure so as to yield a continuous spectrum with wave functions that do not vanish at infinity. One way of doing this is to replace the single-particle harmonic-oscillator potential with a realistic finite collective potential, such as a Woods-Saxon well. Then the single-particle spectrum has both a discrete part and a continuous part. Next it is necessary to generalize the above shell-model calculational procedure in order to permit the calculation of continuum N-particle shell-model wave functions. The asymptotic behavior of such wave functions yields the scattering amplitude from which the cross section can be computed.

A number of detailed procedures for carrying out such calculations have been discussed by Feshbach,[3] MacDonald and Meckjian,[4] Bloch and Gillet,[5] Weidenmüller,[6] Weidenmüller and Dietrich,[7] Glöckle, Hüfner, and Weidenmüller,[8] and Romo.[9] Using Feshbach's projecton-operator theory,[3] cross-section calculations have been carried out by Lemmer and Shakin,[10] Lovas,[11] Afnan,[12] and Payne.[13]

Such calculations are subject to a number of limitations:

(a) The N-particle basis states can have at most one nucleon in a continuum state. This may in some circumstances constitute an undue restriction on the shell-model basis.

(b) It is difficult to antisymmetrize the wave function with respect to the continuum nucleon, particularly when more than one channel is open.

(c) A separate complete shell-model calculation is required at every energy at which the cross section is required. This can become very laborious, particularly when many resonances are involved.

(d) Only single-channel calculations have been possible so far; that is, only elastic scattering and radiative absorption cross sections below the threshold for nonelastic nucleon channels have been calculated.

To overcome these limitations we have undertaken a study of the application of Wigner's R-matrix theory[14-17] to the calculation of shell-model cross sections. In this method the single-particle states are again calculated for a Woods-Saxon potential but now the additional requirement is imposed that the logarithmic radial derivatives of the single-particle states with given l, j have a certain fixed real value (boundary condition) at a channel radius a beyond the range of U and V. The complete set of boundary conditions for all channels gives us an infinite complete discrete single-particle spectrum, just as in the case of the harmonic oscillator. We can then carry through steps 2 through 5 of the ordinary bound-state shell-model procedure described above. The resulting spectrum $E_{\mu JM}$ and eigenfunctions $|\mu JM\rangle$ constitute the spectrum of R-matrix states, their energies, and wave functions.

The true continuum wave function is then obtained by expansion in terms of the orthogonal set of R-matrix states. In this way the continuum part of the calculation is separated from the shell-model calculation of the R-matrix states.

This method does overcome some of the limitations inherent in the methods that employ single-particle continuum wave functions. The size of the shell-model basis is limited only by the size of the problem that can be handled computationally. Each R-matrix state can be fully antisymmetrized, as in the bound-state shell-model calculations. A single set of R-matrix states can yield an adequate expansion of the true wave function over a wide range of energies, so that only one shell-model calculation needs to be performed within that energy range. Cross sections for any number of open channels are easily computed. This involves only the calculation of the surface overlaps of the R-matrix wave functions with those of each of the open reaction channels.

The R-matrix theory has long been useful for the parametrization of resonance cross sections and for their statistical analysis. Specific dynamical content of R-matrix resonance parameters was in-

troduced in the calculation of strength functions from the optical model by Lane, Thomas, and Wigner[18] and in Robson's analysis of isobaric analog resonances.[19] The use of R-matrix methods for the solution of coupled-channel models of nuclear reactions was proposed by Haglund and Robson[20] and studied in greater detail by Buttle.[21]

While the use of R-matrix theory for shell-model calculations yields the advantages outlined above, it also entails some problems and difficulties. The most serious of these is the familiar question of whether the results of R-matrix calculations depend on the choice of channel radii and boundary conditions. Such questions arise because in practice it is not possible to expand the wave function in the complete infinite set of R-matrix states, but only in terms of a finite incomplete set, and because such partial R-matrix expansions do not converge uniformly in a. To overcome this difficulty, Tobocman and Nagarajan,[22] Tobocman,[23] and Garside and Tobocman[24] have proposed generalizations of the R-matrix theory, and these were further studied by Lane and Robson.[25] These authors have noted that Wigner's channel radius a fulfills two separate functions. First, a defines a finite "interior" region within which the Hamiltonian has a complete discrete R-matrix spectrum. Secondly, a defines the boundary of the region in which the wave function is expanded in terms of R-matrix states, and at which this expansion is fitted to the exterior channel wave function. By allowing channel radii to assume different values for these different functions, the convergence difficulty could be ameliorated, either by treating the additional channel-radius values as free parameters or by optimizing their choice according to variational principles.

We choose a different approach. Retaining a single Wigner-Eisenbud channel radius for each channel, we calculate a finite number of R-matrix states and include the slowly convergent contribution of the remaining states in the "background R matrix" which is calculated from the collective part of the nuclear Hamiltonian. We verify the channel-radius independence of the resulting cross sections by calculating cross sections for several values of channel radii.

In addition to testing the channel-radius independence of the method, we demonstrate the ease of nonelastic cross-section calculations and the effect of complete antisymmetrization of the wave function. For this purpose we have calculated the simplest kind of a problem which illustrates all of the above features. This is the case of two identical neutrons in the field of an inert core. For the sake of definiteness we chose the parameters appropriate to the elastic and inelastic scattering of a neutron by ^{17}O. We proceed to present the details of the method in terms of this specific case in Secs. II–VI. Conclusions and application to other cases will be discussed in Sec. VII.

II. SINGLE-PARTICLE PROBLEM

A. Potential

We begin by considering the motion of a single neutron in a spherically symmetric potential U whose radial dependence is given by

$$U(r) = V_r \rho(r) + V_{so}\left(\frac{\hbar}{\mu c}\right)^2 \vec{l}\cdot\vec{s}\,\frac{1}{r}\frac{d\rho}{dr}, \tag{4a}$$

where

$$\rho(r) = (1+e^{-(r-R)/a})^{-1} \tag{4b}$$

and

$$R = r_0 A^{1/3} + r_1, \tag{4c}$$

and where we have chosen the particular numerical values

$$r_0 = 1.16 \text{ fm}, \quad r_1 = 0.6 \text{ fm}, \quad a = 0.938 \text{ fm}, \quad V_r = 42.4 \text{ MeV}, \quad V_{so} = 9.60 \text{ MeV}. \tag{4d}$$

The potential was cut off at $r = 7.0$ fm. This potential with $A = 17$ has two bound states above the p shell: a $1d_{5/2}$ state at -4.146 MeV and a $2s_{1/2}$ state at -3.266 MeV. These correspond to the $\frac{5}{2}^+$ ground state and the $\frac{1}{2}^+$ first excited state in ^{17}O. The phase shifts generated by this potential were computed and their properties have been discussed in detail.[26]

B. R Function

If we were interested only in the single-neutron-potential scattering problem, the numerical solution for the bound states and the phase shifts would yield all the observable consequences of the problem. However, since we will want to use the single-particle wave functions for the solution of a two-neutron problem, we now proceed to discuss the R-function solution of the potential scattering problem.

In order to express the neutron wave function in terms of the R function, we must assign a channel radius $a \geq 7$ fm and a boundary-condition value B_l for each partial wave.[27] Then the R function R_{lj} can be defined in terms of the logarithmic derivative f_{lj} at a of the radial part of the wave function ϕ_{lj} which satisfies the Schrödinger equation with the potential U and is regular at the origin; thus

$$R_{lj} = (f_{lj} - B_l)^{-1}, \tag{5a}$$

$$f_{lj} = \frac{r}{u_{lj}} \frac{du_{lj}}{dr}\bigg|_{r=a}, \tag{5b}$$

and

$$u_{lj} = r\phi_{lj}/i^l Y_{lm}(\hat{r}). \tag{5c}$$

Clearly, f_{lj} and hence R_{lj} are defined for all positive and negative energies. At positive energies, R_{lj} is related to the scattering phase shift δ_{lj} by the relation

$$\tan(\delta_{lj} + \phi_l) = P_l R_{lj}/(1 - S_l^0 R_{lj}), \tag{6}$$

where S_l^0, P_l, and ϕ_l are the shift function, the penetrability function, and the hard-sphere phase shift at a, as defined in Ref. 15. Alternatively, we may write

$$\$_{lj} = e^{2i\delta lj} = e^{-2i\phi_l} \frac{1 - (S_l^0 - iP_l)R_{lj}}{1 - (S_l^0 + iP_l)R_{lj}}. \tag{7}$$

The great virtue of the R function is that it can be expanded into terms corresponding to the eigenfunctions of the Schrödinger equation with the potential U, subject to the boundary condition B_l on the radial logarithmic derivative at a:

$$R_{lj} = \sum_n^{\infty} (\gamma_{nlj}^{SP})^2/(E_{nlj}^{SP} - E), \tag{8}$$

where the E_{nlj}^{SP} are the discrete real eigenvalues and the γ_{nlj}^{SP} are related to real radial parts u_{nlj} of the corresponding eigenfunctions ϕ_{nlj} evaluated at $r = a$:

$$\gamma_{nlj}^{SP} = (\hbar^2/2Ma)^{1/2} u_{nlj}(a). \tag{9}$$

The pole terms in the sum of Eq. (8) will play the crucial role in constructing the scattering resonances of both the one-neutron and then the two-neutron problems. However, within a restricted energy range we do not need to know all pole parameters, but only those that contribute to the formation of resonances within the energy range of interest. Nor are we able, in practice, to calculate all terms of the series. Unfortunately this series (8) converges extremely slowly, so that no set of finite terms gives a good approximation of R_{lj}. For this reason it is essential that R_{lj} be represented as

$$R_{lj} = R_{lj}^{\infty} + \sum_{n=1}^{N_{lj}} \frac{(\gamma_{nlj}^{SP})^2}{E_{nlj}^{SP} - E}, \tag{10}$$

where now the sum is taken only over the N_{lj} eigenstates which must be calculated individually from the Schrödinger equation. The contribution of the remaining resonances is contained in the "distant pole" contribution R_{lj}^{∞} which is calculated from

$$R_{lj}^{\infty} = R_{lj}^{(\text{exact})} - \sum_{n=1}^{N_{lj}} \frac{(\gamma_{nlj}^{SP})^2}{E_{nlj}^{SP} - E}. \tag{11}$$

The exact R function $R_{lj}^{(\text{exact})}$ is calculated from Eqs. (5), using the exact wave function obtained by numerical integration of the potential scattering problem. In practice this procedure is useful only within an energy range in which all important energy variations of R are produced by the finite sum. Within that range, the object is to approximate R_{lj}^{∞} by a constant. For greater precision R_{lj}^{∞} can be fitted by a linear or other simple function of the energy without seriously affecting the calculational method. The test of the validity of this method of calculating R_{lj} is to see whether the resulting cross sections are independent of the choice of channel radius a both in the single-particle problem and later in the two-neutron problem. For this purpose, we will compare cross sections calculated with channel radii set at 7 and 10 fm.

Besides specifying the potential and a channel radius, we must also specify boundary-condition values B_l. For reasons that will become apparent later, we choose for B_0 the logarithmic derivative at a of the $2s_{1/2}$ bound single-particle state of the potential U at -3.266 MeV, and for B_2 we choose the logarithmic derivative at a of the $1d_{5/2}$ bound state of U at -4.146 MeV (see Table I). In this way we assure that these two bound states of U are identical to the corresponding R-function states. The remaining boundary conditions may be chosen arbitrarily for our problem. We adopt for these the convenient choice $B_l = -l$, which is the logarithmic derivative of the zero-energy solution of the zero-potential wave equation. Wherever a boundary condition is not used to make an R-function state coincide with a bound state it may be assigned any negative value. Positive values may lead to unstable calculations.[28]

C. Potential Scattering Cross Sections

The scattering cross section due to the potential U (4) was calculated by a numerical-integration

TABLE I. Boundary values for $a = 7$ and 10 fm.

l	B_l(7 fm)	B_l(10 fm)
0	−2.8621	−4.0888
2	−3.9210	−5.1537

method. As examples, the total cross sections of $s_{1/2}$, $p_{3/2}$, and $d_{3/2}$ waves are shown by curves in Figs. 1(a)–1(c). Next, the R-matrix procedure of Sec. II B was carried through using channel radii $a=7$ and $a=10$ fm. The resulting cross sections are shown as points in Fig. 1.

In doing the R-matrix calculation, the logarithmic derivatives as determined by the bound states of the potential are listed in Table I. The energies of the R-matrix states included in the finite sum of Eq. (10) for the case $a=7$ fm are shown in Fig. 2. The familiar shell structure of the single-particle levels is apparent also in the positive-energy region, although the gaps between shells are less pronounced than in the case where the shells are bound in the Woods-Saxon potential.[29]

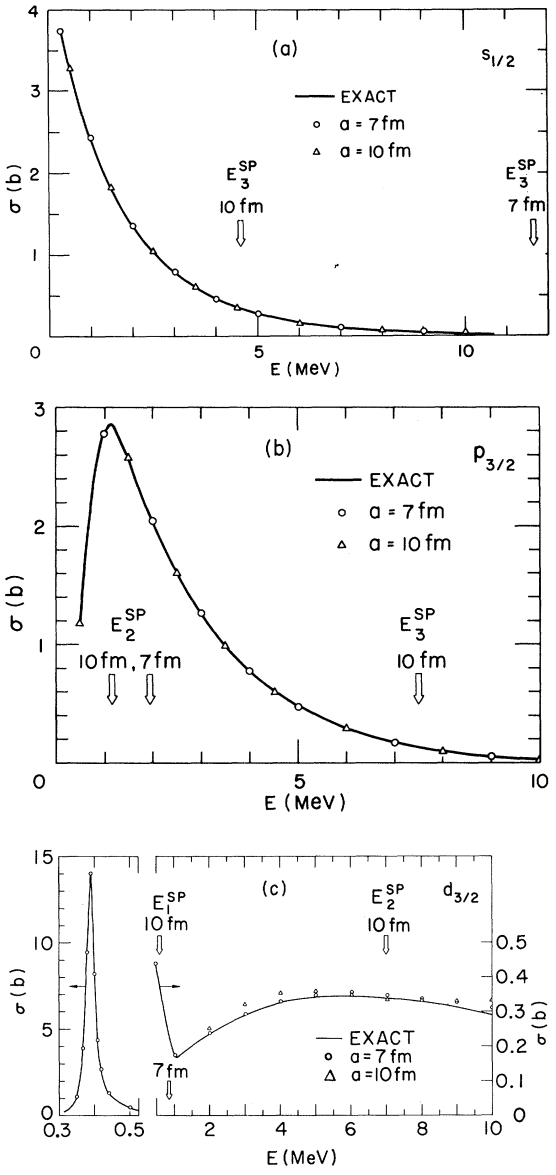

FIG. 1. (a) Single-particle neutron potential scattering cross sections for the $s_{1/2}$ wave. The exact cross section is compared with the R-function results for channel radius $a=7$ and 10 fm. R-function-state energies E_n^{SP} are shown by arrows. (b) Same as (a) for the $p_{3/2}$ wave. E_3^{SP} for $a=7$ fm is at 19.7 MeV. (c) Same as (a) for the $d_{3/2}$ wave. Below 1 MeV the $a=10$ fm. R-function cross section agrees with the exact result.

Table II contains the values of the R-function energies and reduced widths for the $s_{1/2}$, $p_{3/2}$, and $d_{3/2}$ waves. The distant-pole contributions as calculated by Eq. (11) are also shown in the table.

Next, the s functions of Eq. (7) were calculated, and from them the cross sections

$$\sigma_{lj}=\pi\lambda\!\!\!^{-2}|1-S_{lj}|^2, \tag{12}$$

which are plotted as points in Fig. 1, together with the exact cross sections as solid curves. In order to illustrate relations of the R-function poles and resonances, the energies of the R-function states are indicated by arrows.

We see that the R-function method with $a=7$ fm yields excellent results over the entire energy range. A small error in the R-function d-wave cross section for $a=10$ fm is taken as an indication that, for more precise results with such large channel radii, a larger number of R-function states must be included in the sum of pole terms of Eq. (10). This is entirely reasonable, since Table II shows that the $a=10$-fm calculation includes states up to 20 MeV, while the $a=7$-fm calculation includes all states up to 40 MeV. As a matter of fact, the agreement is excellent below 5 MeV.

We see also that while R-function energies vary a great deal with changing channel radius, cross sections are quite independent of the choice of radius when the distant-pole contribution is correctly taken into account. The R-function poles are not always closely related to the resonances. For example, there are no resonances in the s-wave cross sections near the R-function pole positions. However the $p_{3/2}$ resonance at 1.2 MeV and the $d_{3/2}$ resonance at 0.39 MeV are both associated with R-function states. These points have been discussed elsewhere.[26]

III. INDEPENDENT-PARTICLE STATES

From the single-neutron states satisfying the boundary conditions defined in the last section, we now construct independent two-neutron states which will serve as the basis for the shell-model calculation of the next section. To simplify the notation we label the single-particle states by Greek letters α, β, γ, ...:

$$|\alpha\rangle = |n_\alpha l_\alpha j_\alpha m_\alpha\rangle , \tag{13a}$$

$$E_\alpha^{SP} = E_{n_\alpha l_\alpha j_\alpha}^{SP} , \text{ (single-particle state)} , \tag{13b}$$

where, as before, n_α is the principal quantum number of $|\alpha\rangle$, and l_α, j_α, m_α are its orbital and total angular momenta and the z projection of the latter.

The two-neutron states are products of two states $|\alpha\rangle$, $|\beta\rangle$ coupled to total angular momentum J,M and having parity π. They will be labeled either by $|\alpha\beta JM\pi\rangle$ or by the letters p,p', etc.:

$$|p\rangle = |\alpha_p \beta_p J_p M_p \pi_p\rangle = \sum_{m_\alpha m_\beta} \langle j_\alpha m_\alpha j_\beta m_\beta | J_p M_p\rangle \{|\alpha\rangle|\beta\rangle\}_A$$

(two-particle state), (14)

where $\{\ \}_A$ indicates antisymmetrization of the product with respect to the particle coordinates. The energy of the two-particle state is defined to be

$$E_p^{IND} = E_{\alpha\beta JM\pi}^{IND} = E_\alpha^{SP} + E_\beta^{SP} - E_{1d_{5/2}} , \tag{15}$$

where $E_{1d_{5/2}}$ is the single-particle energy of the $\frac{5}{2}^+$ ground state of ^{17}O.

It is clear that the states $|p\rangle$ are orthonormal so-

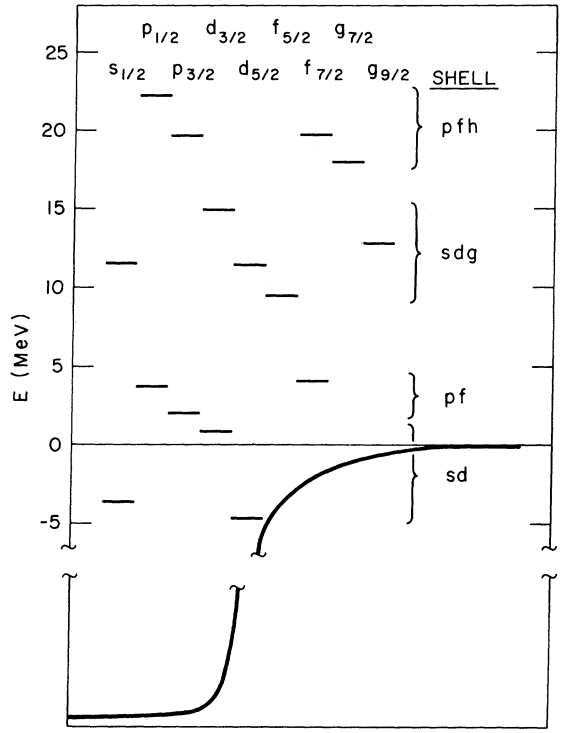

FIG. 2. The R-function energies E_n^{SP} for channel radius $a=7$ fm.

TABLE II. Single-particle R-function parameters.

		$a=7$ fm			$a=10$ fm		
l_j	n	E_{nlj}^{SP}	γ_{nlj}^{SP}	R_{lj}^{∞}	E_{nlj}^{SP}	γ_{nlj}^{SP}	R_{lj}^{∞}
$s_{1/2}$	2	−3.66	−0.458	0.0570	−3.66	−0.108	0.0587
	3	11.58	0.942		4.60	0.565	
	4	36.45	−0.973		15.53	−0.651	
$p_{1/2}$	2	3.73	−0.994	0.0668	1.86	−0.629	0.0797
	3	22.25	1.052		8.97	−0.745	
$p_{3/2}$	2	1.97	−0.932	0.0731	1.13	−0.538	0.0844
	3	19.70	1.076		7.50	0.776	
$d_{3/2}$	1	0.83	0.374	0.0551	0.51	0.131	0.0552
	2	14.91	−0.854		7.06	−0.527	
	3	39.12	0.930		18.07	0.608	
$d_{5/2}$	1	−4.71	0.255	0.0584	−4.71	0.0425	0.0601
	2	11.42	−0.821		5.70	−0.475	
	3	34.78	0.942		15.58	0.609	
$f_{5/2}$	1	9.47	0.716	0.0693	6.25	0.542	0.0714
	2	25.54	−0.948		12.97	−0.617	
$f_{7/2}$	1	4.03	0.511	0.0745	3.50	0.261	0.0806
	2	19.74	−0.980		9.19	−0.692	
$g_{7/2}$	1	18.06	0.822	0.0588	10.25	0.620	0.0592
	2	39.40	−0.919		20.70	−0.614	
$g_{9/2}$	1	12.80	0.644	0.0637	9.19	0.506	0.0661
	2	31.49	−0.947		16.11	−0.603	

lutions of the Schrödinger equation for two noninteracting neutrons moving under the influence of the potential U and satisfying the boundary conditions B_l at $r=a$ for either neutron. We can use these solutions to define an independent-particle R matrix. This requires the introduction of the concept of a channel, that is, the definition of two fragments. In our case the fragments considered are a neutron and ^{17}O in one of the two bound single-neutron states of our model; that is, either the $\frac{5}{2}^+$ ground state or the $\frac{1}{2}^+$ first excited state. We define the channel wave functions to be products of one of these two bound-state single-neutron wave functions and the angular part of the free-neutron wave function coupled to a total channel angular momentum JM:

$$|c\rangle = |\alpha l j JM\pi\rangle = \sum_{\substack{m_\alpha m \\ m_l m_s}} \langle l m_l \tfrac{1}{2} m_s | j m\rangle \langle j_\alpha m_\alpha j m | JM\rangle \times |\alpha\rangle Y_{l m_l}(\Omega) S_{\frac{1}{2} m_s}\,, \tag{16}$$

where $Y_{l m_l}(\Omega)$ is the spherical harmonic of the angular coordinates of the unbound neutron and $S_{\frac{1}{2} m_s}$ is its spin function, and $|\alpha\rangle$ can be either of the two bound single-neutron states of ^{17}O.

To obtain independent-particle-model R-matrix γ coefficients $\gamma^{\rm IND}_{p,c}$, we calculate the overlaps of the channel wave functions $|c\rangle$ with the two-neutron wave functions $|p\rangle$, with the latter evaluated for one of the neutron radial coordinates having the value of the channel radius $r_1=a$:

$$\gamma^{\rm IND}_{p,c} = (2\hbar^2/2Ma)^{1/2} \langle c|p\rangle_{r_1=a}\,, \tag{17}$$

where

$$\langle c|p\rangle = \sum_M \langle \alpha_c l_c j_c J_c M_c \pi_c | \beta_p \gamma_p J_p M_p \pi_p\rangle_{r_1=a} \tag{18}$$

and where the extra factor of $\sqrt{2}$ arises from the fact that either of the two antisymmetrized neutrons may have an overlap with the channel wave function; that is there is a second contribution from $r_2=a$. In other words, Eq. (17) compensates for the fact that our channel wave function (16) is not explicitly antisymmetrized.

Because we have chosen our boundary conditions so that the first two single-neutron R-function states $|1d_{5/2}\rangle$ and $|2s_{1/2}\rangle$ are identical to the $\frac{5}{2}^+$ and $\frac{1}{2}^+$ bound states of ^{17}O which define the two-neutron channels $|c\rangle$ of interest, the evaluation of the $\gamma^{\rm IND}_{pc}$ coefficients is exceedingly simple. The orthogonality of the R-function states $|\alpha\rangle$ assures that $\gamma^{\rm IND}_{pc}$ vanishes unless either $|\beta_p\rangle$ or $|\gamma_p\rangle$ in Eq. (14) is the same as $|\alpha_c\rangle$ which may be either $|1d_{5/2}\rangle$ or $|2s_{1/2}\rangle$. Furthermore, assuming that $|\beta_p\rangle = |\alpha_c\rangle$, the orthogonality of the vector coupling coefficients assures that $\gamma^{\rm IND}_{pc}$ vanishes unless the channel neutron quantum numbers (l_c, j_c) are identical to $(l_\gamma j_\gamma)$ of the state $|\gamma_p\rangle$. Of course the total angular momentum (J,M) and parity π of the channel $|c\rangle$ and the two-neutron R-matrix state $|p\rangle$ must also agree. The nonvanishing independent-particle $\gamma^{\rm IND}_{pc}$ are then just identical to the single-neutron $\gamma^{\rm SP}_{nlj}$ of Eq. (9):

$$\gamma^{\rm IND}_{pc} = \delta_{\alpha_c \beta_p} \delta_{l_c l_\gamma} \delta_{j_c j_\gamma} \gamma^{\rm SP}_{n\gamma l_\gamma j_\gamma}. \tag{19}$$

We can now write down the independent-particle R matrix

$$R^{\rm IND}_{cc'} = R^{{\rm IND},\infty}_{cc'} + \sum_p \frac{\gamma^{\rm IND}_{pc}\gamma^{\rm IND}_{pc'}}{E^{\rm IND}_p - E}\,. \tag{20}$$

If the sum is extended over all two-neutron states $|p\rangle$, then $R^{{\rm IND},\infty}$ vanishes. In that case we find from Eq. (19) that the diagonal elements $R^{\rm IND}_{cc}$ are identical to the corresponding single-neutron R function R_{ij} evaluated at a shifted energy according to Eq. (15):

$$R^{\rm IND}_{cc}(E) = R_{ij}(E + E_{1d_{5/2}} - E_\alpha)\,, \tag{21}$$

where

$$|c\rangle = |\alpha l j JM\pi\rangle\,.$$

If we now cut off the sums of $R^{\rm IND}$ and R_{ij} in the same way, we are also left with the same remaining distant-pole contribution for the diagonal elements:

$$R^{{\rm IND},\infty}_{cc}(E) = R^{\infty}_{ij}(E + E_{1d_{5/2}} - E_\alpha)\,. \tag{22}$$

Next we turn to the off-diagonal part of $R^{\rm IND}$, which connects the channels in which ^{17}O is left in its ground state to the channel in which it is in its first excited state. According to Eq. (19) only one two-neutron state $|p\rangle$ contributes, namely, the one in which one neutron is in the $1d_{5/2}$ ground state and the other is in the $2s_{1/2}$ first excited state:

$$R^{\rm IND}_{cc'} = \gamma^{\rm IND}_{pc}\gamma^{\rm IND}_{pc'}/(E_p - E)\,, \tag{23}$$

where

$$|\alpha_c\rangle = |\beta_p\rangle = |1d_{5/2}\rangle\,,$$
$$|\alpha_{c'}\rangle = |\gamma_p\rangle = |2s_{1/2}\rangle\,, \tag{24}$$

or vise versa. Since there are no other off-diagonal contributions, there are no contributions from distant resonances, and we see that $R^{{\rm IND},\infty}$ is diagonal. This is rigorously so in our model and does not depend on any additional physical assumption,

TABLE III. Numbers of independent-particle configurations.

	sd through *pfh* shells		*sdgi* shell
J^π	$\gamma^{\mathrm{IND}}=0$	$\gamma^{\mathrm{IND}}\neq 0$	$\gamma^{\mathrm{IND}}\neq 0$
0^-	9	3	1
0^+	17	4	2
1^-	24	9	1
1^+	18	7	5
2^-	32	10	2
2^+	37	11	7
3^-	32	10	2
3^+	28	9	7
4^-	27	7	1
4^+	30	8	6
5^-	19	3	1
5^+	15	4	4
6^-	10	2	0
6^+	12	2	2
7^-	0	0	0
7^+	3	1	1
Total	223	90	42

such as random signs, etc.

On the other hand, the strict diagonality of $R^{\mathrm{IND},\infty}$ is a consequence of the j-j vector coupling scheme of angular momenta, that we have adopted above. If one adopts the channel-spin labeling scheme, in which the target angular momentum is first coupled to the neutron spin to form the channel spin S, then $R^{\mathrm{IND},\infty}$ does have some trivial off-diagonal elements that connect states with different channel spins. It is therefore important to realize that one cannot arbitrarily assume vanishing off-diagonal elements of $R^{\mathrm{IND},\infty}$ in all channel labeling schemes. The channel-spin wave functions are given in terms of the j-j-coupling channel wave functions of Eq. (16) by

$$|c\rangle = |\alpha l S J M\pi\rangle = \sum_j \hat{j}\,\hat{S} W(l\tfrac{1}{2} J j_\alpha; jS) |\alpha l j J M\pi\rangle , \tag{25}$$

where $\hat{j} = (2j+1)^{1/2}$ and similarly for $\hat{S}$, and W is the Racah coefficient. Correspondingly, the γ coefficients and distant-pole contribution become

$$\gamma^{\mathrm{IND}}_{pc} = \delta_{\alpha\beta}\delta_{ll_\gamma}\delta_{jj_\gamma}\hat{j}\,\hat{S} W(l\tfrac{1}{2} J j_\alpha; jS)\gamma^{\mathrm{SP}}_{n\gamma l_\gamma j_\gamma} , \tag{26}$$

where

$$R^{\mathrm{IND},\infty}_{cc'} = \delta_{\alpha\alpha'}\delta_{ll'}\sum_j \hat{j}^2\hat{S}\hat{S}' W(l\tfrac{1}{2} J j_\alpha; jS) \times W(l\tfrac{1}{2} J j_\alpha; jS') R^{\infty}_{ij} , \tag{27}$$

where $S, S' = j_\alpha \pm \frac{1}{2}$.

Our actual computations have been carried out on the channel-spin scheme[15] and include the contributions of all the single-particle states through the *sdgi* shell. The numbers of the resulting antisymmetrized two-neutron states are listed in Table III according to their total angular momentum and parity. The first column lists the 223 two-neutron states with neutrons through the *pfh* shell, but with neither neutron in either the $|1d_{5/2}\rangle$ ground state or in the $|2s_{1/2}\rangle$ first excited states. Since these states have all vanishing $\gamma^{\mathrm{IND}}_{pc}$, they will clearly not contribute to the independent-particle-model R matrix, but they will be included in the later shell-model calculation. The second column lists the 90 antisymmetrized states with one neutron in $|1d_{5/2}\rangle$ or $|2s_{1/2}\rangle$ and the other neutron in any one of the states through the *pfh* shell. Listed separately in the third column are the 42 states with one neutron in $|1d_{5/2}\rangle$ or $|2s_{1/2}\rangle$ and the other in the *sdgi*

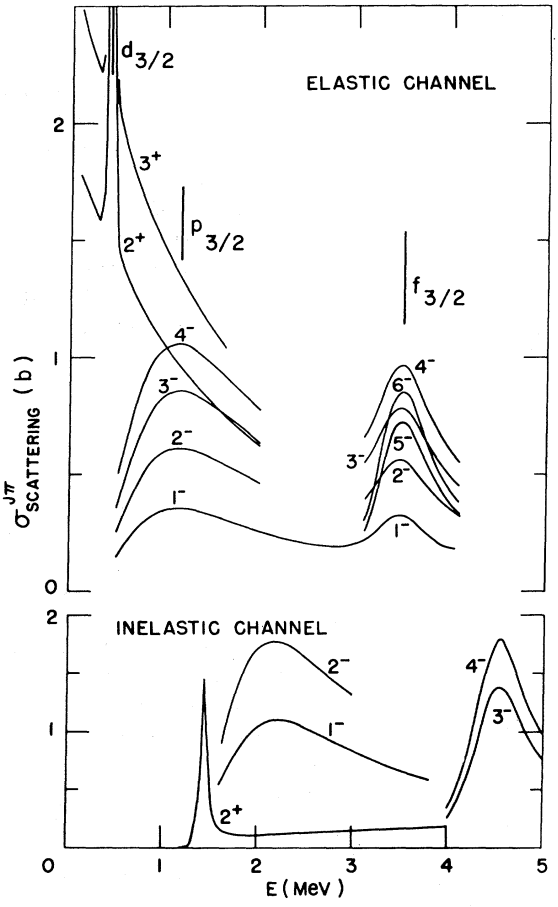

FIG. 3. Elastic scattering cross sections σ_p^{IND} according to the independent-particle model in the elastic (ground-state) and inelastic (first-excited-state) channels of ^{17}O. The cross sections for each J^π peak together at the $d_{3/2}$, $p_{3/2}$, and $f_{7/2}$ single-particle resonances indicated by vertical lines. The same resonances appear in the inelastic channel, shifted by the threshold energy.

TABLE IV. Independent-particle R-matrix parameters.

$n_1l_1j_1;n_2l_2j_2$	p	E_p^{IND}	$\gamma_p^{IND}(\alpha lS)$ (033)	(111)
$J^\pi=0^-$				
$(2s_{1/2}2p_{1/2})$	1	4.78		−0.994
$(1d_{5/2}1f_{5/2})$	3	9.47	0.716	
$(2s_{1/2}3p_{1/2})$	6	23.29		1.052
$(1d_{5/2}2f_{5/2})$	8	25.54	−0.948	
$J^\pi=0^+$				
$(1d_{5/2})^2$	1	−4.71	0.361	
$(2s_{1/2})^2$	2	−2.62		−0.648
$(1d_{5/2}2d_{5/2})$	5	11.42	−0.821	
$(2s_{1/2}3s_{1/2})$	7	12.62		0.942
$(1d_{5/2}3d_{5/2})$	18	34.78	0.942	
$(2s_{1/2}4s_{1/2})$	19	37.49		−0.974

shell. Energies E_p and γ_{pc} values for the 32 states in columns 2 and 3 having $J^\pi=0\pm,1\pm$ are given in Table IV and the values of $R^{IND,\infty}$ for these J^π are given in Table V.

Using the complete results for the 132 states in columns 2 and 3 of Table III, we constructed the independent-particle R matrices, and from them obtained by standard methods the independent-particle-model cross sections.

Since there is no inelastic process, one obtains only elastic scattering cross sections in the ground-state and first-excited-state channels but no inelastic transitions between them. Furthermore, the resonances that appear are just the single-particle resonances of Fig. 1. These independent-particle-model scattering cross sections are shown in Fig. 3 separated according to J^π. The $d_{3/2}$, $p_{3/2}$, and $f_{7/2}$ single-neutron resonances appear at about 0.5, 1.2, and 3.5 MeV in the elastic channel and are shifted up by the threshold energy (1.045 MeV) in the inelastic channel.

TABLE V. Constant part of $R^{\infty}_{cc'}$ ($a=7.0$ fm).

	(αlS)				
$J^\pi=0^-$	(133)	(211)			
(133)	0.0693				
(211)		0.0668			
$J^\pi=0^+$	(122)	(200)			
(122)	0.0584				
(200)		0.0570			
$J^\pi=1^-$	(112)	(132)	(133)	(210)	(211)
(112)	0.0731				
(132)		0.0743	0.001 12		
(133)		0.001 12	0.0695		
(210)				0.0710	0.002 97
(211)				0.002 97	0.0689
$J^\pi=1^+$	(122)	(123)	(143)	(201)	(221)
(122)	0.0582	0.000 80			
(123)	0.000 80	0.0554			
(143)			0.0588		
(201)				0.0570	
(221)					0.0551

IV. SHELL-MODEL R MATRIX

The independent-particle R matrix yields only single-particle resonances. In order to obtain more complicated compound-nucleus states, we must introduce a neutron-neutron interaction V which we choose to have the form

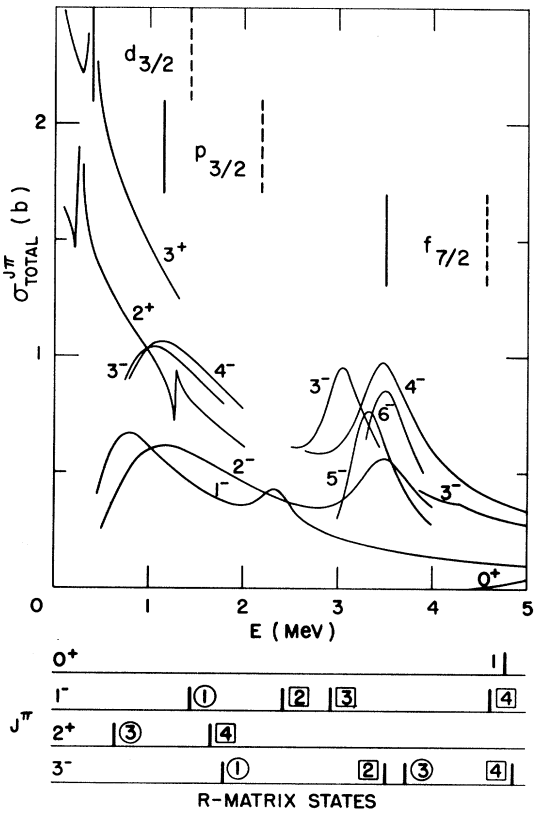

FIG. 4. Total shell-model scattering cross sections for neutrons bombarding ^{17}O is its ground state, separated according to J^π. The positions of the $d_{3/2}$, $p_{3/2}$, and $f_{7/2}$ single-particle resonances in the elastic and inelastic channels are indicated by solid and broken vertical lines, respectively. The positions of the shell-model R-matrix-state energies are indicated at the bottom for $J^\pi=0^+$, 1^-, 2^+, 3^-, numbered according to their ordering starting from the lowest state. A circle around the number indicates that the predominant configuration of the state has one neutron in $|d_{5/2}\rangle$. A square indicates that predominantly one neutron is in $|2s_{1/2}\rangle$. A plain number indicates that in the principal configuration neither neutron is in $|d_{5/2}\rangle$ or $|2s_{1/2}\rangle$.

$$V(1,2) = (V_0 + V_s P_s)\delta(\vec{r}_1 - \vec{r}_2)\,, \tag{28a}$$

where

$$V_0 = -582.3 \text{ MeV/fm}^3\,, \qquad V_s = 314.4 \text{ MeV/fm}^3\,, \tag{28b}$$

where $P_s = \frac{1}{4}(1 - \vec{\sigma}_1 \cdot \vec{\sigma}_2)$ is the projection operator for the singlet states. This potential, which was originally suggested by Brown, Castillejo, and Evans[30] to fit the low-lying spectra of p-shell nuclei, has been applied to elastic scattering calculations by a number of authors.[10-13]

With this interaction our shell-model Hamiltonian then becomes

$$H = \sum_{i=1}^{2} [K(i) + U(i)] + V(1,2)\,, \tag{29}$$

where $K(i)$ is the single-neutron kinetic-energy operator and $U(i)$ is the single-particle potential of Eq. (4). The shell-model R-matrix states X_μ with energies E_μ are the solutions of the Schrödinger equation with the shell-model Hamiltonian (29) subject to the boundary condition B_i which were specified in Sec. II.

These shell-model R-matrix states are obtained as expansions in the independent two-neutron states, Eq. (14),

$$X_\mu = \sum_p C_{\mu p} |p\rangle\,, \tag{30}$$

where the coefficients $C_{\mu p}$ are the elements of the eigenvectors of the matrix of H in the independent-particle basis $|p\rangle$ and the energies E_μ are its eigenvalues

$$\sum_{p'} \langle p|H|p'\rangle C_{\mu p'} = E_\mu C_{\mu p}\,. \tag{31}$$

This procedure works, of course, only when the sums are limited to a finite set of two-particle configurations $|p\rangle$. We require therefore an assumption that is shared by all shell-model calculations; namely, that the interaction $V(1,2)$ mixes a configuration $|p\rangle$ into the shell-model state X_μ only if $|E_p^{\rm IND} - E_\mu|$ is less than some finite mixing range D_V. Then, if all states $|p\rangle$ with energies $E_p^{\rm IND}$ up to some E_p (max) are included in the sums of Eqs. (30) and (31), the shell-model assumption implies that all X_μ with energies E_μ up to

$$E_\mu(\max) = E_p(\max) - D_V \tag{32}$$

are correctly computed.

In our calculations the mixing range D_V is less than 5 MeV. The matrix elements of V connecting states more than 5 MeV apart have magnitudes that are 3 orders of magnitude less than those of the diagonal matrix elements of V. Since we are interested in cross sections in the energy range of 0–5 MeV, we should therefore retain all configurations up to 10 MeV. Actually our shell-model calculations of Eq. (31) include all configurations in columns 1 and 2 of Table III, that is those having neutrons up through the *pfh* shell as shown in Fig. 2. These constitute all the configurations up to 20 MeV when the neutron channel radius a is 7 fm and up to 10 MeV when a is 11 fm. As seen from Table III the maximum dimension of the calculated shell-model matrices is 48 in the case of $J^\pi = 2^+$.

Using this set of configurations, the shell-model R matrix for $E < 5$ MeV can be represented by

$$R_{cc'} = R^\infty_{cc'} + \sum_\mu \frac{\gamma_{\mu c}\gamma_{\mu c'}}{E_\mu - E}\,, \tag{33}$$

where

$$\gamma_{\mu c} = \sum_p C_{\mu p}\gamma^{\rm IND}_{pc}\,. \tag{34}$$

Because of Eq. (26) only the 90 states listed in the second column of Table III contribute to the sums of Eq. (34), but all 313 configurations listed in the first two columns of Table III contribute to the determination of the E_μ and the $C_{\mu p}$ through the solutions of Eq. (31). Therefore the R matrix (33) does reflect the entire shell-model configuration space up through the *pfh* shell, including many configurations with two neutrons having positive single-particle energies. The latter are difficult to include in some other computation schemes.[3-13]

Next, we must consider the configurations which are excluded from the shell-model calculation (31). These produce R-function states that are not contained in the sum of Eq. (33), and their effect must therefore be included in $R^\infty_{cc'}$. Let us consider the contribution of a certain set $\{s\}$ of highly excited configurations $|p\rangle$, all of whose E_p are greater than E_p(max). They will yield the following partial contribution to R^∞ that can be obtained from an expanded shell-model calculation of the type of Eq. (34):

$$R_{cc'}\{s\} = \sum_\mu \sum_{p,p' \text{ in } \{s\}} \frac{C_{\mu p}C_{\mu p'}\gamma^{\rm IND}_{pc}\gamma^{\rm IND}_{p'c'}}{E_\mu - E}\,. \tag{35}$$

If all the states occuring in this sum have $E_\mu - E \gg D_V$, that is to say, if the mixing range D_V is small compared with the distance from the excluded configurations to the energy range of interest, then we may make the approximation

$$E_\mu \cong E_p^{\mathrm{IND}}. \tag{36}$$

Applying also the orthogonality relations

$$\sum_\mu C_{\mu p} C_{\mu p'} = \delta_{pp'}\ , \tag{37}$$

we obtain

$$R_{cc'}\{s\} \cong \sum_{p \text{ in } \{s\}} \frac{\gamma_{pc}^{\mathrm{IND}} \gamma_{pc'}^{\mathrm{IND}}}{E_p^{\mathrm{IND}} - E}\ . \tag{38}$$

This is identical to the contribution of the same set of configurations $\{s\}$ to $R_{cc'}^{\mathrm{IND},\infty}$. We conclude therefore upon summing over all sets $\{s\}$ that

$$R_{cc'}^{\infty} \cong R_{cc'}^{\mathrm{IND},\infty}. \tag{39}$$

The background R matrix obtained in this way is again diagonal except for trivial off-diagonal spin-flip terms. One also obtains a diagonal background R matrix by invoking the assumption of random and uncorrelated signs of the $\gamma_{\mu c}$ coefficients. We have *not* used this assumption here, but rather we have relied on the common assumption that shell-model states have negligible contributions from very distant independent-particle configurations. In the last section we shall discuss how this assumption can be relaxed.

We have included the contributions of all configurations with neutrons above the *pfh* shell by including their effects in R^∞ as prescribed by Eqs. (30), (22), and (11). In order to improve the accuracy of the calculation, particularly for the larger choices of channel radius, we have approximated by a constant only the contributions to R^∞ from above the *sdgi* shell. For the contributions of the *sdgi* shell configurations listed in column 3 of Table III, we have used $R^{\mathrm{IND},\infty}$ as an energy-dependent contribution to R^∞.

V. MATRIX ELEMENTS AND PARITY SELECTION RULE

Details of the calculation of the two-body matrix elements $\langle p|V|p'\rangle$ occuring in Eq. (31) are discussed in the Appendix where they are expressed as radial integrals multiplied by vector coupling coefficients.

It is shown in the Appendix that for zero-range interactions the two-body antisymmetrized matrix elements $\langle p|V|p'\rangle$ vanish for unnatural-parity states having $\pi = (-)^{J+1}$. This selection rule, which has previously been known for diagonal matrix elements,[31] is here shown to hold also for the off-diagonal elements. Consequently, the independent-particle states of unnatural parity do not spread over the R-matrix states, and hence the contribution to the cross section of the unnatural-parity states is unaffected by the presence of zero-range two-body forces. While this selection rule does not hold exactly for finite-range potentials, we may still expect that the unnatural-parity matrix elements are reduced compared with the natural-parity elements. If we suppose that a partial selection rule also holds for finite-range off-diagonal matrix elements, we must conclude that the spreading of independent two-neutron or two-proton unnatural-parity states is reduced. Therefore we may expect reductions in the strength of the imaginary optical potential for the unnatural-parity states, resulting in parity and J dependences of the nuclear strength function.[32] The latter effect has been seen experimentally.[33]

VI. S MATRIX AND CROSS SECTIONS

Having obtained the R matrix, we calculate the S matrix by standard R-matrix inversion procedures according to the formula[14-17]

$$S = \Omega P^{1/2}(1 - RL^0)^{-1}(1 - RL^{0*})P^{-1/2}\Omega\ , \tag{40}$$

where Ω, P, and L^0 are the diagonal matrices given in Ref. 15. This procedure is best adapted to cases in which the number of asymptotic channel states for each J^π is less than the number of independent-particle configurations, In cases of many channel states but few configurations and energy-independent R^∞, the level-matrix inversion procedure may be more efficient.[14-17]

From the S matrix we calculate total and inelastic cross sections by

$$\sigma_{\mathrm{tot}}^{J\pi} = 2\pi\lambda\!\!\!^{-2} g_J \sum_{lS} [1 - \mathrm{Re}(S_{cc})] \tag{41}$$

and

$$\sigma_{\mathrm{inel}}^{J\pi} = \pi\lambda\!\!\!^{-2} g_J \sum_{ll'} \sum_{SS'} |S_{c'c}|^2\ , \tag{42}$$

where $c = (1d_{5/2})lSJ^\pi$, and $c' = (2s_{1/2})l'S'J^\pi$. For neutron scattering by oxygen in the energy range 0–5 MeV, it is sufficient to include orbital angular momenta up to 4. Channel spins are 2 and 3 in the elastic channel ($\frac{5}{2}^+$), and 0 and 1 in the inelastic channel ($\frac{1}{2}^+$). Thus, the total angular momentum ranges from 0 to 7. Actually, we have carried out calculations of R-matrix constants in 60 different asymptotic channel states $|c\rangle$ and $|c'\rangle$.

A. Resonances

The contributions of the various total angular momenta and parities to the total cross section are shown in Fig. 4. These curves were calculated using a neutron channel radius of 7 fm. For compar-

ison the positions of the single-particle resonances of the independent-particle model of Fig. 3 are indicated by vertical lines. Due to the residual interaction, the natural-parity cross-section resonances are shifted from their independent-particle positions.

The residual interaction also introduces a second sharp 2^+ resonance at 1.3 MeV due to the $d_{3/2}$ wave single-particle resonance in the inelastic channel. In the continuum shell-model theories, the appearance of such a resonance is ascribed to "continuum-continuum interactions."[7,8] In our calculation the 1.3-MeV 2^+ resonance arises from configuration mixing of the independent-particle R-matrix states. In the independent-particle model, the 2^+ state having ^{17}O in its $2s_{1/2}$ excited state plus a $1d_{3/2}$ neutron has a vanishing γ_{pc} in the elastic channel (which is a quasibound state in the inelastic channel). Therefore, this state does not appear as a resonance in the independent-particle ground-state channel, but it does cause a sharp quasibound state resonance at 1.4 MeV in the inelastic channel. The residual interaction mixes the $1d_{5/2}$ ground state plus $1d_{3/2}$ neutron configuration into this $2s_{1/2}$-$1d_{3/2}$ quasi-bound state, giving it a finite γ_{pc} in the elastic channel and resulting in the second sharp 2^+ resonance at 1.3 MeV. The 2.3 MeV 1^- and 4.3 MeV 3^- resonances are of the same type.

A third type of resonance is the very weak 0^+ peak at about 5 MeV. This is due to the two-particle excitation $(1d_{3/2})^2$ which is weakly coupled to the ground-state channel by the residual interaction. Such a resonance might be called a doorway state, although in our model it is the most complicated kind of a compound-nucleus configuration leading to a resonance. Since there are no more complicated states, we might call this state a closed doorway.

For comparison with the resonances, the positions of the R-matrix states are indicated at the bottom of Fig. 4 and in Table VI. As has already been pointed out in the single-particle case, only a few R-matrix states correspond to scattering resonances.[26] Here we see the same situation in the two-particle case. For example, there are four 1^- R-matrix states in the energy range up to 5 MeV but only two 1^- resonances. The number of resonances does in fact appear to be equal to the

TABLE VI. Shell-model R-matrix parameters for channels in order of increasing l and increasing S for same l.

		$\gamma_{\mu c}$ (el)					$\Sigma\gamma_{\mu c}{}^2$(el)	$\gamma_{\mu c'}$(inel)		$\Sigma\gamma_{\mu c'}{}^2$
J^Π	E	$c=1$	2	3	4	5		$c'=1$	$c'=2$	(inel)
0^-	4.78	−0.99					0.980	0.0		0.0
0^+	4.99	0.14					0.020	−0.07		0.005
1^-	1.46	−0.901	0.056	0.018			0.815	−0.042	−0.055	0.005
	2.23	0.113	0.273	0.083			0.094	−0.456	−0.472	0.431
	2.94	−0.048	−0.328	−0.089			0.118	−0.483	−0.381	0.378
	4.62	0.005	0.034	0.006			0.001	−0.675	0.714	0.965
1^+	0.83	−0.096	0.361	0.0			0.140	0.0	0.0	0.0
	1.88	0.0	0.0	0.0			0.0	0.0	0.374	0.140
2^-	1.97	−0.822	−0.440	0.0	0.0		0.869	0.0	0.0	0.0
	3.02	0.0	0.0	0.0	0.0		0.0	−0.932	0.0	0.869
	3.73	0.469	−0.877	0.0	0.0		0.989	0.0	0.0	0.0
	4.03	0.0	0.0	0.474	0.193		0.262	0.0	0.0	0.0
2^+	0.66	−0.033	0.180	−0.316	0.017	0.008	0.134	0.020	−0.044	0.002
	1.68	0.030	0.021	−0.045	−0.016	−0.008	0.004	−0.224	0.291	0.135
3^-	1.81	−0.551	−0.740	0.013	0.013		0.852	0.011	0.023	0.001
	3.51	0.353	−0.205	0.345	0.253		0.350	0.070	0.102	0.015
	3.57	−0.710	0.545	0.165	0.117		0.842	0.008	0.011	0.001
	4.86	−0.042	0.093	−0.120	−0.055		0.033	0.355	0.336	0.239
3^+	0.83	0.0	−0.236	0.289	0.0	0.0	0.139	0.0	0.0	0.0
4^-	1.97	−0.932	0.0	0.0			0.869	0.0	0.0	0.0
	4.03	0.0	0.370	0.353			0.262	0.0		0.0
4^+	0.32	−0.302	0.187	−0.009	−0.016		0.127	−0.004	−0.014	0.000
5^-	3.83	0.340	0.441				0.310			
6^-	4.03	0.511					0.261			

number of single-particle resonances in all channels of our model. We see total-cross-section resonances corresponding to ground-state single-particle resonances, as well as 2^+, 1^-, 3^- resonances corresponding to single-particle resonances of the first excited state, and finally we see a 0^+ resonance corresponding to a two-particle one-hole state relative to ^{17}O.

B. Antisymmetrization Effects

The total and inelastic scattering cross sections obtained by summing Eq. (41) over J^π,

$$\sigma = \sum_{J^\pi} \sigma^{J^\pi}, \tag{43}$$

are plotted in Fig. 5. The relative magnitude of the total and inelastic cross sections are comparable to the measured ratio,[34] which suggest that the strength of the residual interaction is approximately correct.

In order to see the effect of using antisymmetrized wave functions, we have calculated these same cross sections without antisymmetrization. The R matrix is calculated by the formula

$$R^{(0)} = \tfrac{1}{2}(R^{(+)} + R^{(-)}), \tag{44}$$

where $R^{(-)}$ is the antisymmetrized R matrix and $R^{(+)}$ is the R matrix obtained from the symmetrized wave functions of the Appendix. The factor $\frac{1}{2}$ is due to the fact that so far as $R^{(+)}$ and $R^{(-)}$ are concerned, the two neutrons are indistinguishable in the channels, while for $R^{(0)}$ the channel wave functions must be defined with distinguishable neutrons [see discussion below Eq. (17)].

The resulting total and inelastic cross sections are shown in Fig. 6. They differ from Fig. 5 by the appearance of more resonance peaks resulting from the additional resonance states contributed by $R^{(+)}$. The increased coupling of channels through these new states is reflected in an inelastic cross section that is about twice as large as in the antisymmetrized case. The parity selection rule of the Appendix does not hold, and the effect of each independent-particle state is spread over many more resonances than the case when the Pauli principle is obeyed.

C. Channel Radius Effects

To check the consistency of our calculational method, in particular the procedure for determin-

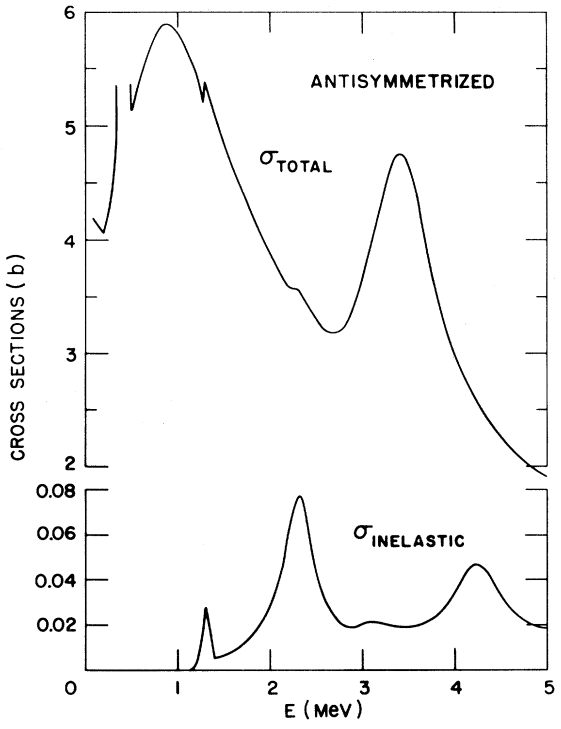

FIG. 5. Total and inelastic shell-model cross sections for neutrons scattered by ^{17}O, calculated with antisymmetrized wave functions.

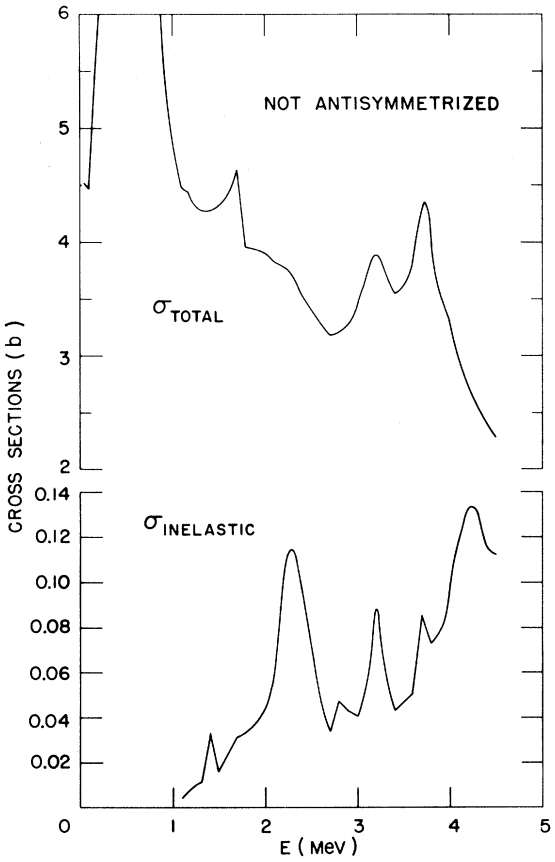

FIG. 6. Same as Fig. 5 but calculated without antisymmetrization of the wave functions.

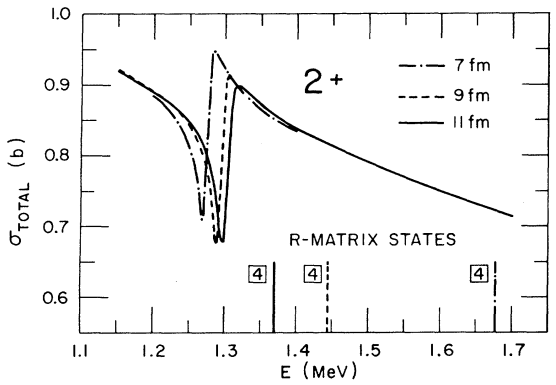

FIG. 7. The 2^+ resonance at 1.3 MeV calculated for channel radii $a=7$, 9, and 11 fm. The energy of the fourth 2^+ R-matrix state responsible for this resonance is indicated for each value of a by a vertical line.

ing R^∞, we have performed the above calculations for neutron channel radii of 7, 8, and 11 fm. Detailed results are shown in Figs. 7 and 8. In Fig. 7, the 1.3-MeV 2^+ resonance in the total cross section is plotted for the three choices of channel radii. At the bottom of the figure are indicated the corresponding positions of the R-matrix state responsible for this resonance. We see that as a is shifted from 7 to 11 fm the R-matrix state shifts by over 300 keV from 1.68 to 1.37 MeV. In contrast, the resonance curve is almost unchanged. The actual computed resonance shift is about 30 keV *in the opposite direction* from the R-matrix shift. This small reverse shift arises from the fact that in this calculation the single-neutron bound R-function states were normalized to unity in the space $r < a$. The resulting a-dependent normalization of the independent-particle states produces a-dependent shell-model R-matrix states, resulting in the observed small a dependence of the cross section. A similar small shift in the 1^- resonances is shown in Fig. 8.

This effect can be removed by giving the bound single-particle R-function states the correct bound-state normalization regardless of channel radius. Subsequently the shell-model R-matrix states have to be normalized to unity within the interior space $r < a$, and these correctly normalized R-matrix states must be used for the calculation of the $\gamma_{\mu c}$. It is not clear whether this additional labor in normalizing all R-matrix states is warranted in practice. Another way of minimizing the normalization error is to choose the channel radii a as large as possible consistent with keeping the size of the shell-model problem within managable bounds. Figures 7 and 8 shows that the cross sections calculated from single-particle bound states normalized in the interior converges rapidly with increasing channel radius.

VII. CONCLUSION

We conclude that the usual R-matrix method does present a convenient method for carrying out nuclear-structure calculation in the continuum. We have demonstrated its advantages in minimizing the required number of shell-model calculations, in permitting complete antisymmetrization of the wave functions, in permitting the use of arbitrarily large shell-model bases and in carrying through multichannel calculations. The difficulty of possible channel-radius dependence of the cross section has been seen to be removed by the correct compu-

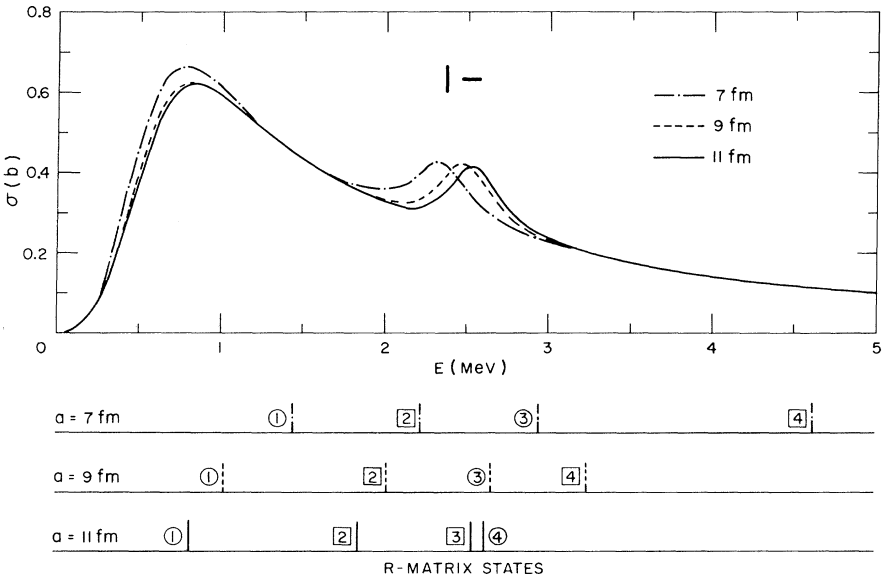

FIG. 8. The 1^- resonances at 0.9 and 2.5 MeV calculated for channel radii $a=7$, 9, and 11 fm. Energies of relevant R matrix states are shown.

tation of the distant-pole contribution R^{∞}.

The method described and applied here to a core-plus-two-neutron system can be immediately generalized to more complicated systems. For example, in a three-nucleon problem, or a two-nucleon–one-hole problem, one must first carry out a shell-model calculation for the target system to determine its bound states. From there on, the calculation proceeds analogous to the two-neutron case. Such calculations will be facilitated by use of (l,j) quantum numbers to specify asymptotic channel states, rather than the channel-spin classification employed here. This permits separate specification of boundary conditions B_{lj} for each (l,j) wave. Each single-particle state contributing to a bound target state must be assigned its "natural" boundary condition as in the case of the $1d_{5/2}$ and $2s_{1/2}$ states of the above two-neutron problem. Only if two single-particle states with the same angular momentum quantum numbers but different principal quantum numbers contribute to bound residual states, does the present method require modification.

Finally, direct reactions can be introduced into our calculational procedure by replacing the separate single-particle models for each of the channels by a coupled-channel model which correctly represents the direct transitions between collective states. Employing the subtraction procedure of Eq. (11) in matrix form, one then obtains off-diagonal elements in R^{∞} which correspond to off-diagonal contributions of the distant R-matrix states.

APPENDIX. MATRIX ELEMENTS AND SELECTION RULES

A two-neutron state $|p\rangle_{(0)}$ without symmetry properties is written in terms of the single-particle states $|\alpha(1)\rangle$ of neutron 1 and $|\beta(2)\rangle$ of neutron 2 as follows:

$$|p\rangle_{(0)} = |p(\alpha\beta)\rangle_{(0)} = \sum_{m_\alpha m_\beta} \langle j_\alpha m_\alpha j_\beta m_\beta | JM\rangle \, |\alpha(1)\rangle \, |\beta(2)\rangle . \tag{A1}$$

The corresponding symmetrized state will be denoted by $|p\rangle_{(+)}$, while the antisymmetrized state is denoted by $|p\rangle_{(-)}$. These are given by the expression

$$|p\rangle_{(\pm)} = \frac{K^{(\pm)}_{\alpha\beta}}{\sqrt{2}} \sum_{m_\alpha m_\beta} \langle j_\alpha m_\alpha j_\beta m_\beta | JM\rangle [\,|\alpha(1)\rangle|\beta(2)\rangle \pm |\alpha(2)\rangle|\beta(1)\rangle\,] , \tag{A2}$$

where the normalization constants $K^{(\pm)}_{\alpha\beta}$ have the values[31]

$$\begin{aligned} K^{(\pm)}_{\alpha\beta} &= 1 && \text{when } \{nlj\}_\alpha \neq \{nlj\}_\beta \\ &= \frac{1}{\sqrt{2}} \frac{1 \pm (-)^{J+1}}{2} && \text{when } \{nlj\}_\alpha = \{nlj\}_\beta . \end{aligned} \tag{A3}$$

The matrix elements of $V(1,2)$ formed with the symmetrized and antisymmetrized states (A2) are expressed in terms of the states $|p\rangle_{(0)}$ of Eq. (A1) by

$$\langle p|V(1,2)|p'\rangle_{(\pm)} = K^{(\pm)}_{\alpha\beta} K^{(\pm)}_{\gamma\delta} [\langle p(\alpha\beta)|V|p'(\gamma\delta)\rangle_{(0)} \pm (-)^{j_\gamma + j_\delta - J} \langle p(\alpha\beta)|V|p'(\gamma\delta)\rangle_{(0)}] . \tag{A4}$$

The δ-function interaction of Eq. (28) yields two contributions to the matrix elements $\langle p|V|p'\rangle_{(0)}$ that have been given by Newby and Konopinsky[35] as follows: The spin-independent contribution is

$$\begin{aligned} \langle p(\alpha\beta)|V_0 \delta(\vec{r}_1 - \vec{r}_2)|p'(\gamma\delta)\rangle_{(0)} = {} & \frac{V_0 G}{2\hat{J}^2} \hat{j}_\alpha \hat{j}_\beta \hat{j}_\gamma \hat{j}_\delta \langle j_\alpha {}^{1/2} j_\beta {}^{-1/2}|J0\rangle \langle j_\gamma {}^{1/2} j_\delta {}^{-1/2}|J0\rangle \\ & \times \left\{ (-)^{(j_\alpha + j_\gamma + l_\alpha + l_\gamma + 1)} + \frac{[j_\alpha{}^2 + (-)^{(j_\alpha + j_\beta + J)} \hat{j}_\beta{}^2][\hat{j}_\gamma{}^2 + (-)^{(j_\gamma + j_\delta + J)} \hat{j}_\delta{}^2]}{4J(J+1)} \right\} . \end{aligned} \tag{A5}$$

The singlet contribution is

$$\langle p(\alpha\beta)|V_s P_s \delta(\vec{r}_1 - \vec{r}_2)|p'(\gamma\delta)\rangle_{(0)} = \frac{V_s G}{2\hat{J}^2} \hat{j}_\alpha \hat{j}_\beta \hat{j}_\gamma \hat{j}_\delta (-)^{(j_\alpha + j_\gamma + l_\alpha + l_\gamma + 1)} \langle j_\alpha j_\beta {}^{-1/2}|J0\rangle \langle j_\gamma j_\delta {}^{-1/2}|J0\rangle \tag{A6}$$

if $J + l_\alpha + l_\beta$ is even, and zero otherwise. In addition, these matrix elements vanish unless parity is conserved, i.e., unless $l_\alpha + l_\beta + l_\gamma + l_\delta$ is even. We have used the notation

$$\hat{j}_\alpha = (2j_\alpha + 1)^{1/2}$$

and

$$G = \frac{1}{4\pi} \int_0^{a_P} \frac{u_\alpha u_\beta u_\gamma u_\delta}{r^2}\, dr\,,$$

where a_P is the potential cutoff radius beyond which also $V(1,2)$ is set equal to zero.

Substituting these expressions (A5) and (A6) into Eq. (A4), we obtain

$$\langle p|V_0\delta(\vec{r}_1-\vec{r}_2)|p'\rangle_{(\pm)} = K^{(\pm)}_{\alpha\beta}K^{(\pm)}_{\gamma\delta}\frac{V_0G}{2\hat{J}^2}\hat{j}_\alpha\hat{j}_\beta\hat{j}_\gamma\hat{j}_\delta\langle j_\alpha{}^{1/2}j_\beta{}^{-1/2}|J0\rangle\langle j_\gamma{}^{1/2}j_\delta{}^{-1/2}|J0\rangle$$
$$\times\left\{(-)^{j_\alpha+j_\gamma+l_\alpha+l_\gamma+1}[1\mp(-)^{l_\alpha+l_\beta+J}] + (1\pm 1)\,\frac{[\hat{j}_\alpha{}^2+(-)^{j_\alpha+j_\beta+J}\hat{j}_\beta{}^2][\hat{j}_\gamma{}^2+(-)^{j_\gamma+j_\delta+J}\hat{j}_\delta{}^2]}{4J(J+1)}\right\} \tag{A8}$$

and

$$\langle p|V_sp_s\delta(\vec{r}_1-\vec{r}_2)|p'\rangle_{(\pm)} = K^{(\pm)}_{\alpha\beta}K^{(\pm)}_{\gamma\delta}\frac{V_sG}{2\hat{J}^2}j_\alpha j_\beta j_\gamma j_\delta\langle j_\alpha{}^{1/2}j_\beta{}^{-1/2}|J0\rangle\langle j_\gamma{}^{1/2}j_\delta{}^{-1/2}|J0\rangle$$
$$\times(-)^{(j_\alpha+j_\beta+l_\alpha+l_\beta+1)}[1\mp(-)^{l_\alpha+l_\beta+J}]\,\frac{1+(-)^{(l_\alpha+l_\beta+J)}}{2}\,. \tag{A9}$$

We see immediately that both the spin-independent contribution (A8) and the singlet contribution (A9) to the antisymmetrized matrix element $\langle p|V|p'\rangle_{(-)}$ will vanish unless the condition that

$$(l_\alpha + l_\beta + J) \quad \text{is even} \tag{A10}$$

is satisfied. Assuming the zero-spin inert core to have positive parity, this condition implies the selection rule that the matrix elements of V vanish unless

J is even for even-parity states

or

J is odd for odd-parity states.

This selection rule has been previously stated for only the diagonal matrix elements of the two-body δ-function interaction by de-Shalit and Talmi.[31] The only selection rule operating for the matrix elements with symmetrized functions is that they vanish for $J^\pi = 0^+$.

---

*Work performed under the auspices of the U. S. Atomic Energy Commission.

[1]C. Mahaux and H. A. Weidenmüller, *Shell-Model Approach to Nuclear Reactions* (John Wiley & Sons, New York, 1969), and references cited there.

[2]In general, also isobaric spin quantum numbers will be required. We drop these here because our calculations will deal exclusively with neutrons. The extension to systems including protons is straightforward.

[3]H. Feshbach, Ann. Phys. (N.Y.) 5, 357 (1958); 19, 287 (1962).

[4]W. MacDonald and A. Mekjian, Phys. Rev. 160, 730 (1967).

[5]C. Bloch and V. Gillet, Phys. Letters 16, 62 (1965).

[6]H. A. Weidenmüller, Nucl. Phys. 75, 189 (1965).

[7]H. A. Weidenmüller and K. Dietrich, *ibid.* 83, 332 (1966).

[8]W. Glöckle, J. Hüfner, and H. A. Weidenmüller, *ibid.* A90, 481 (1967).

[9]W. J. Romo, Nucl. Phys. A116, 617 (1968).

[10]R. H. Lemmer and C. M. Shakin, Ann. Phys. (N.Y.) 27, 13 (1964).

[11]I. Lovas, Nucl. Phys. 81, 353 (1966).

[12]I. R. Afnan, Phys. Rev. 163, 1016 (1967).

[13]G. L. Payne, Phys. Rev. 174, 1227 (1968).

[14]E. P. Wigner and L. Eisenbud, Phys. Rev. 72, 29 (1947).

[15]A. M. Lane and R. G. Thomas, Rev. Mod. Phys. 30, 257 (1958).

[16]G. Breit, in *Encyclopedia of Physics*, edited by S. Flügge (Springer-Verlag, Berlin, Germany, 1959), Vol. 41/1.

[17]H. B. Willard, L. C. Biedenharn, P. Huber, and E. Baumgartner, in *Fast Neutron Physics*, edited by J. B. Marion and J. L. Fowler (Interscience Publishers, Inc., New York, 1963), Part II, p. 1217.

[18]A. M. Lane, R. G. Thomas, and E. P. Wigner, Phys. Rev. 98, 693 (1955).

[19]D. Robson, Phys. Rev. 137, B535 (1965).
[20]M. E. Haglund and D. Robson, Phys. Letters 14, 225 (1965).
[21]P. J. A. Buttle, Phys. Rev. 160, 719 (1967).
[22]W. Tobocman and M. A. Nagarajan, Phys. Rev. 138, B1351 (1965); 140, B63 (1965).
[23]W. Tobocman, Phys. Rev. 166, 1036 (1968).
[24]L. Garside and W. Tobocman, Phys. Rev. 173, 1947 (1968).
[25]A. M. Lane and D. Robson, Phys. Rev. 178, 1715 (1969).
[26]K. Takeuchi and P. A. Moldauer, preceding paper Phys. Rev. C 2, 920 (1970).
[27]In general it is possible to use separate boundary conditions B_{lj} for each l,j wave. See Sec. VII.
[28]C. Mahaux and H. A. Weidenmüller, Phys. Rev. 170, 847 (1968).
[29]K. Takeuchi and P. A. Moldauer, Phys. Letters 28B, 384 (1969).
[30]G. E. Brown, L. Castillejo, and J. A. Evans, Nucl. Phys. 22, 1 (1961).
[31]A. de Shalit and I. Talmi, *Nuclear Shell Theory* (Academic Press Inc., New York, 1963), Part II, p. 199.
[32]For the relation of the imaginary potential to the strength function, see P. A. Moldauer, Nucl. Phys. 47, 65 (1963).
[33]J. Julian, in *Nuclear Structure Study with Neutrons*, edited by M. N. de Mevergnies, P. Van Assche, and J. Vervier (North-Holland Publishing Company, Amsterdam, The Netherlands, 1966), p. 156.
[34]*Neutron Cross Sections*, compiled by D. J. Hughes and R. B. Schwartz, Brookhaven National Laboratory Report No. BNL-325 (U. S. Government Printing Office, Washington, D. C., 1958), 2nd ed.
[35]N. Newby, Jr., and E. J. Konopinski, Phys. Rev. 115, 434 (1959).